Thermal and Mechanical Properties of Blended Polyimide and Amine-Functionalized Poly(orthosiloxane) Composites

Pallavi Iyer, Maria R. Coleman

Department of Chemical and Environmental Engineering, University of Toledo, 2801 West Bancroft Street, Toledo, Ohio 43606

Received 18 June 2007; accepted 30 October 2007
DOI 10.1002/app.27607
Published online 21 February 2008 in Wiley InterScience (www.interscience.wiley.com).

ABSTRACT: Nanocomposite films were prepared through the blending of polyimide (PI) with octaphenyl silsesquioxane (OPS) and an amino-functionalized analogue, octaaminophenyl silsesquioxane (OAPS), with a solution-casting method. Although the PI–OPS composites showed visible phase separation at 5 wt %, the PI–OAPS composites were transparent with visible phase separation occurring only at 50 wt % OAPS. The interfacial interactions and homogeneity of the composites were characterized with scanning electron microscopy (SEM) and dynamic mechanical analysis. SEM analysis showed a uniform fracture surface for OAPS composites at concentrations up to 20 wt %. Interestingly, OAPS-rich particles with sizes of less than 1 μm were formed within the PI matrix for the 50 wt % composite. The PI–OAPS composites showed higher glass-transition temperatures (T_g's) than the pure PI. The PI–OPS composites showed a T_g lower than that of the pure PI, and this suggested poor interfacial interactions. The slightly enhanced thermal stability of PI–OAPS composites (up to 20 wt %) was attributed to the inherent thermal stability of OAPS at higher temperatures. There were small increases in the modulus and strength for the composites with respect to the base polymer. © 2008 Wiley Periodicals, Inc. J Appl Polym Sci 108: 2691–2699, 2008

Key words: blending; composites; glass transition; polyimides; polysiloxanes

INTRODUCTION

Organic–inorganic polymer nanocomposites have emerged as a class of high-performance materials that combine the multifunctionality of the inorganic nanofiller with the processibility, light weight, and flexibility of the polymer phase.[1] Inorganic nanoparticles can be used to tailor the properties of polymers on a molecular level and can also act as reinforcements within a polymer matrix. The high surface area and surface energy of nanofillers can result in significant improvements in the properties of their polymer composites; however, these properties can also lead to aggregation of these particles within the polymer matrix, thereby affecting the properties of the composite. To overcome this problem, the insoluble nanoparticles are usually incorporated into the polymer matrix by *in situ* polymerization or blending. Many techniques, such as sonication and shear mixing, have been used to improve the blending of nanofillers into polymers and to reduce aggregation.[2] An alternative to blending these insoluble nanofillers within polymer matrices would be to use nanoparticles that could dissolve in solution and hence disperse easily.

Polyhedral oligomeric silsesquioxanes (POSSs) are a class of inorganic molecules with precise three-dimensional cage structures that are soluble and therefore easily dispersible in a polymer matrix. A POSS consists of a Si—O cage formed by tetravalent Si atoms bound to three oxygen atoms and one functional group (R), which gives it unique properties. The R group can be tailored to be inert or reactive with different chemistries depending on the target application. Commonly used T_8-type POSSs with the formula $(RSiO_{1.5})_8$ are cyclopentyl silsesquioxane, octaphenyl silsesquioxane (OPS), and octaepoxy silsesquioxane.[3] POSSs have a size of $\sim$ 1.5 nm and are the basic building blocks of zeolites. The size and regular three-dimensional structure of POSSs suggest that there may be potential for growing these materials within polymer matrices to obtain novel zeolite composite materials.

Recently, a lot of research has focused on the development of such polymer–POSS composites, targeting a wide range of applications. Numerous studies have reported POSS composites with polycarbonate, epoxy, and polyurethane polyimides (PIs) and other widely used industrial polymers.[4–6] PIs have

Correspondence to: M. R. Coleman (macolema@eng.utoledo.edu).

been of particular interest because they can serve a wide range of applications, such as coatings for microelectronic devices, gas-separation membranes, and high-temperature materials. They exhibit good mechanical properties such as tensile strength, modulus, toughness, thermal stability, and high glass-transition temperatures (T_g's).[7] Furthermore, the nanocomposites formed with these polymers have also shown very promising properties; for example, materials such as silica and ceramics, when incorporated into PIs, are known to reduce their coefficient of thermal expansion (CTE) because of the inherently low CTE of the inorganic component.[8] Also, their mixed matrix membranes with zeolite, silica, and carbon molecular sieves have been shown to improve the gas-transport properties of PIs.[9,10] These encouraging properties of PIs led to the investigation of these materials in this study as well.

Property enhancements in a nanocomposite depend largely on the distribution of the nanofiller in the bulk polymer and the interphase between the two.[11,12] A good interphase is one in which the gap between the filler and the bulk polymer matrix is minimum with very little or no property variation. The reactive R groups in POSSs enable either covalent or strong physical interactions with the bulk polymer, thereby reducing such interface issues. Because POSSs are soluble molecular cages, they can be incorporated into the polymer matrix in three different ways: (1) through grafting as a pendant group to a polymer chain, (2) through *in situ* polymerization by covalent binding within the polymer backbone, and (3) by simple blending of a multifunctional POSS within a polymer.

There has been considerable research on grafting POSS into the polymer chain during polymerization or the growth of polymer chains from the surface of the POSS with either a mono- or disubstituted POSS. Lee et al.[8] developed a PI–POSS nanocomposite for low-dielectric applications by incorporating epoxy–POSS into the backbone of the PI during polymerization. A study done by Ni and Zheng[6] on *in situ* polymerized octaamine POSS with epoxy showed a uniform dispersion under transmission electron microscopy even at 10 wt % POSS, suggesting the successful formation of a nanocomposite. Gonzalez et al.[13] adopted a similar *in situ* polymerization technique to incorporate diamine-substituted POSS into Kapton to increase its resistance to atomic oxygen attack. Zhao and Schirald[4] studied the effect of functionalization of POSS on the compatibility and mechanical properties of polycarbonate by melt blending. Composites of POSS with polymers have shown enhanced T_g, thermal stability (decomposition temperature), density, and oxidation resistance. Although there have been several studies on the *in situ* polymerization and grafting of POSS into different polymer matrices, there has been very little reported on the effect of blending POSS with polymers, especially in PIs.[4,14] This blending approach may be more suitable for commercial applications.

In this article, the impact of blending octaphenyl and octaaminophenyl POSS on the thermal and mechanical properties of a 2,2-bis(3,4-dicarboxyphenyl)-hexafluoropropane dianhydride (6FDA)/4,4′-diaminediphenylmethane (MDA) PI is discussed. The study describes the effect of a favorably functionalized and unfunctionalized POSS on the properties of the PI composite. For this work, a T_8 octaphenyl POSS (OPS) was functionalized with amine moieties and incorporated into the 6FDA–MDA PI. The properties of these composites were studied with scanning electron microscopy (SEM), dynamic mechanical analysis (DMA), thermogravimetric analysis (TGA), and Instron tensile testing.

EXPERIMENTAL

Materials and methods

OPS was purchased from Aldrich (Milwaukee, WI). The PI 6FDA–MDA (Fig. 1) was synthesized with the standard chemical imidization method. The dianhydride, 6FDA, was purchased from Clariant, Inc. (Charlotte, NC), and the diamine MDA was purchased from Aldrich. The monomers 6FDA and MDA were purified by sublimation before use. *N*,*N*-Dimethylacetamide (DMAc) was purified by distillation over calcium hydride under a nitrogen atmosphere. Tetrahydrofuran (THF) was freshly prepared by distillation over sodium/benzophenone under a nitrogen atmosphere before use.

Instrumentation and characterization

A Digilab (Canton, MA, USA) FTS 4000 Fourier transform infrared (FTIR) apparatus was used to characterize functional groups on POSS after each functionalization step. ^{1}H-NMR spectra were recorded at the Instrumentation Center at the University of Toledo on a Varian (Palo Alto, CA, USA) VXRS-400 MHz spectrometer with acetone-d_6 as the solvent and tetramethylsilane as the internal standard.

The molecular weight of the synthesized 6FDA–MDA PI was determined with a Shimadzu (Columbia, MD, USA) SCL-10A VP series gel permeation chromatography (GPC) system with a 300 × 7.8 mm

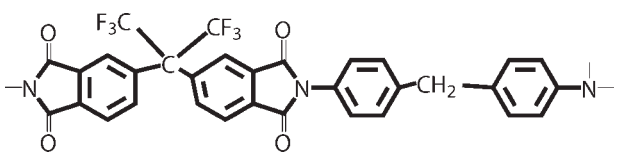

Figure 1 Structure of one repeat unit of 6FDA–MDA PI.

Phenomenex Phenogel column (5 μ, 10^4 Å). Chromatography-grade THF (purchased from Aldrich) was used as the eluting solvent. The sample was prepared by the dissolution of 1–2 mg/mL PI in GPC-grade THF. The standard GPC start-up and operating procedure was adopted. The sample solution was filtered *in vacuo* to remove any particulate foreign objects that were likely to block the column. Molecular weights were determined on the basis of a calibration curve obtained from polystyrene standards in THF.

All testing of the bulk polymer and composites was performed on films cast from a THF solution. Thermal and mechanical properties such as the T_g and storage modulus of pure PI and PI–POSS composites were determined with a dynamic mechanical analyzer (Q800, TA Instruments, Shaumburg, IL, USA) at a heating rate of 2°C/min and a frequency of 1 Hz. Rectangular strips up to 5 mm wide, 0.1 mm thick, and 16 mm long were mounted on a DMA tension clamp, and the experiment was run with a temperature ramp frequency sweep program.

A TA Instruments Q50 thermogravimetric analyzer was used to determine the thermal stability and degradation of the POSS and composites at a heating rate of 5°C/min under a nitrogen atmosphere. Sample weights were between 5 and 10 mg.

The strength, Young's modulus, and strain at yield of the pure PI and composites were tested on an Instron universal tensile tester (Norwood, MA, USA) at a drawing rate of 1 mm/min at room temperature. Dog-bone samples were cut with a die according to ASTM Standard 638. The sample thickness and gauge length were measured with a caliper and kept constant for all samples.

The morphology of the fracture surface of the composite films was observed with an FEI Nova 200 (Hillsboro, OR, USA) scanning electron microscope equipped with an X-ray EDAX UTW (energy dispersive x-ray ultra thin window) detector at the EMAL Instrumentation Center (University of Michigan). The samples were prepared via snapping under liquid nitrogen and coating with gold before mounting.

Synthesis of octaaminophenyl silsesquioxane (OAPS)

The phenyl groups on OPS were functionalized with amines with a two-step reaction mechanism shown in Scheme 1.[15,16] The nitration of POSS was done with the reaction method developed by Huang et al.[17] For this reaction, 10 g of OPS was charged to a round-bottom flask and kept in a water/ice bath at 0°C. Then, fuming nitric acid (50 mL) was added in parts and stirred for 0.5 h at 0°C and for 20 h at room temperature. The reaction mixture was poured over ice to obtain a faint yellow precipitate. This precipitate was filtered, washed with distilled water, and dried at 70°C to obtain octanitrophenyl silsesquioxane (ONPS).

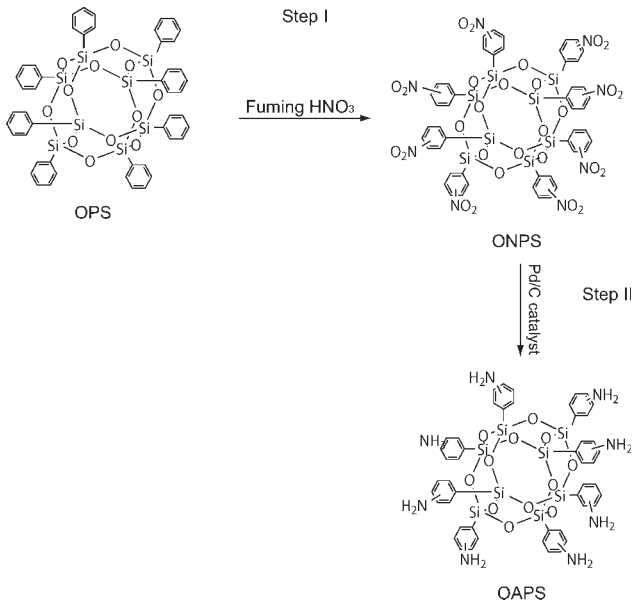

Scheme 1 Reaction scheme for the functionalization of OPS to OAPS.

The catalytic hydrogenation of ONPS was done with Huang's method with a slight modification.[17] For this reaction, ONPS (5 g) was charged to a 300-mL, three-necked flask with a condenser and under a nitrogen atmosphere. Freshly distilled THF (40 mL) was added via a syringe and stirred until the ONPS completely dissolved. A 5 wt % Pd/C catalyst (0.61 g) and 40 mL of triethylamine were added. After this, the mixture was heated to 60°C, and 98% formic acid (4.4 mL) was added dropwise over a period of 2 h with a pressure-equalizing dropping funnel. The reaction was carried out for 14 h and filtered over a bed of Celite, and 40 mL of ethyl acetate was added to the filtrate and extracted with distilled water (20 mL, 3×). The organic phase was collected and dried over sodium sulfate and was precipitated into 1 L of hexanes to obtain a pale yellow precipitate, which was collected by filtration and dried *in vacuo* for 2 days. The product was dissolved in a THF/ethyl acetate (30:50) mixture and precipitated in hexane for further purification. The resulting compound was dried *in vacuo* for 3 days to obtain a white powder of pure OAPS.

Preparation of the nanocomposite films

Before the formation of composites, the PI (6FDA–MDA) was synthesized with a well-established condensation polymerization method.[18] For this reaction, the diamine MDA (10 mmol, 1.98 g) was charged to a three-necked flask with a condenser under nitrogen. Distilled DMAc (50 mL) was added,

an equimolar amount of the dianhydride 6FDA (10 mmol, 4.44 g) was added, and the mixture was stirred for 4 h at room temperature to form a poly (amic acid). To this, an equimolar mixture of triethylamine and acetic anhydride was added, and the temperature was increased to 50°C and held there for 1 h. Final imidization was achieved by the heating of the mixture to 100°C for 30 min, during which cyclical dehydration of the poly(amic acid) took place. The PI was precipitated into 1 L of methanol, filtered, and dried at 60°C for 2 days and at 260°C *in vacuo* for 16 h to remove the residual solvent. The structure of PI and the formation of an imide bond were confirmed with FTIR. The molecular weights were determined with GPC in THF (weight-average molecular weight = 66,754, number-average molecular weight = 47,152, weight-average molecular weight/number-average molecular weight = 1.416).

The pure 6FDA–MDA film, made for comparison with the composites, was solution-cast from THF. For this procedure, the PI was dissolved in THF, filtered to remove impurities, and cast in a glass Petri dish. The dish was kept in a glove bag under a THF environment until all the solvent evaporated. The film was dried at 80°C for 2 days and at 260°C *in vacuo* for 16 h. To prepare PI–OAPS composite films, PI and OAPS were dissolved separately in THF, blended for 15 min, and solution-cast in a glass Petri dish. Composite films of PI–OPS were prepared in methylene chloride (as OPS is insoluble in THF) to determine the effect of functionalization on the appearance and mechanical properties of the composite. All composites were dried in a fashion similar to that used for the pure PI.

RESULTS AND DISCUSSION

FTIR and NMR spectroscopy

The formation of ONPS and OAPS after each functionalization step was confirmed with FTIR as shown in Figure 2. The FTIR spectrum of ONPS shows the formation of two distinct N=O peaks at 1348 and 1530 cm^{-1}. Furthermore, when ONPS was hydrogenated to form OAPS, the two N=O peaks disappeared, and a new broad peak characteristic of N—H in the amines appeared at 3467 cm^{-1}. A prominent Si—O—Si peak at about 1100 cm^{-1} was observed for OPS, ONPS, and OAPS.

The successful formation of ONPS and OAPS was also confirmed with ^{1}H-NMR spectroscopy. Because all the protons on the phenyl ring in ONPS are identical, a triplet corresponding to four protons was observed at a chemical shift of 8.7 ppm in the NMR spectrum (not shown) of ONPS. This chemical shift of the phenyl protons shifted to 9 ppm on hydrogenation, and a new peak corresponding to two protons of $—NH_2$ appeared at 4.2 ppm for OAPS (not shown). Therefore, FTIR and NMR analysis confirmed the modification of OPS to OAPS.

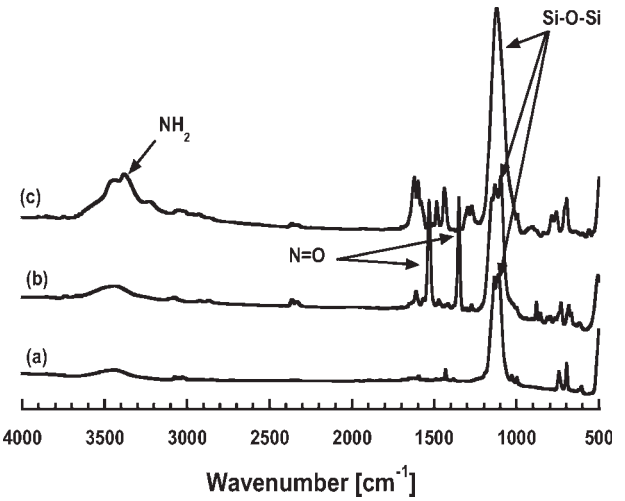

Figure 2 Changes in the FTIR spectrum of (a) OPS on nitration and hydrogenation to (b) ONPS and (c) OAPS.

Polymer synthesis and film formation

Films of pure PI and its blends with OAPS were cast with THF as the solvent, whereas blends of PI with OPS were cast in methylene chloride as OPS was insoluble in THF. Prominent phase separation was observed in PI–OPS blends as the OPS separated out from the polymer phase during film formation and drying, resulting in a nonhomogeneous film. This suggested that there were unfavorable interactions between OPS and PI. Therefore, the OPS was converted to OAPS, as it was expected that the amine functionalities would interact favorably with the 6FDA–MDA and improve the compatibility of POSS with the polymer phase. The pure 6FDA–MDA film was pale yellow and transparent. Films formed by the blending of 0–50 wt % OAPS in PI were also transparent, and their color changed from pale yellow to brown with increasing OAPS concentration. This color change was more prominent for films with OAPS loadings between 20 and 50 wt %. Also, all the films with an OAPS concentration beyond 30 wt % were fairly brittle. The optical transparency and appearance of the blended samples indicated that OAPS was incorporated into the polymer matrix with no visible phase separation. Thus, the functionalization of OPS with amine groups facilitated its blending with the PI over the concentration range studied.

The morphology of the fracture surfaces of pure PI and its composites and the aggregation of OAPS to form larger nanosized particles were probed with SEM. Micrographs of the pure PI and 10, 20, and

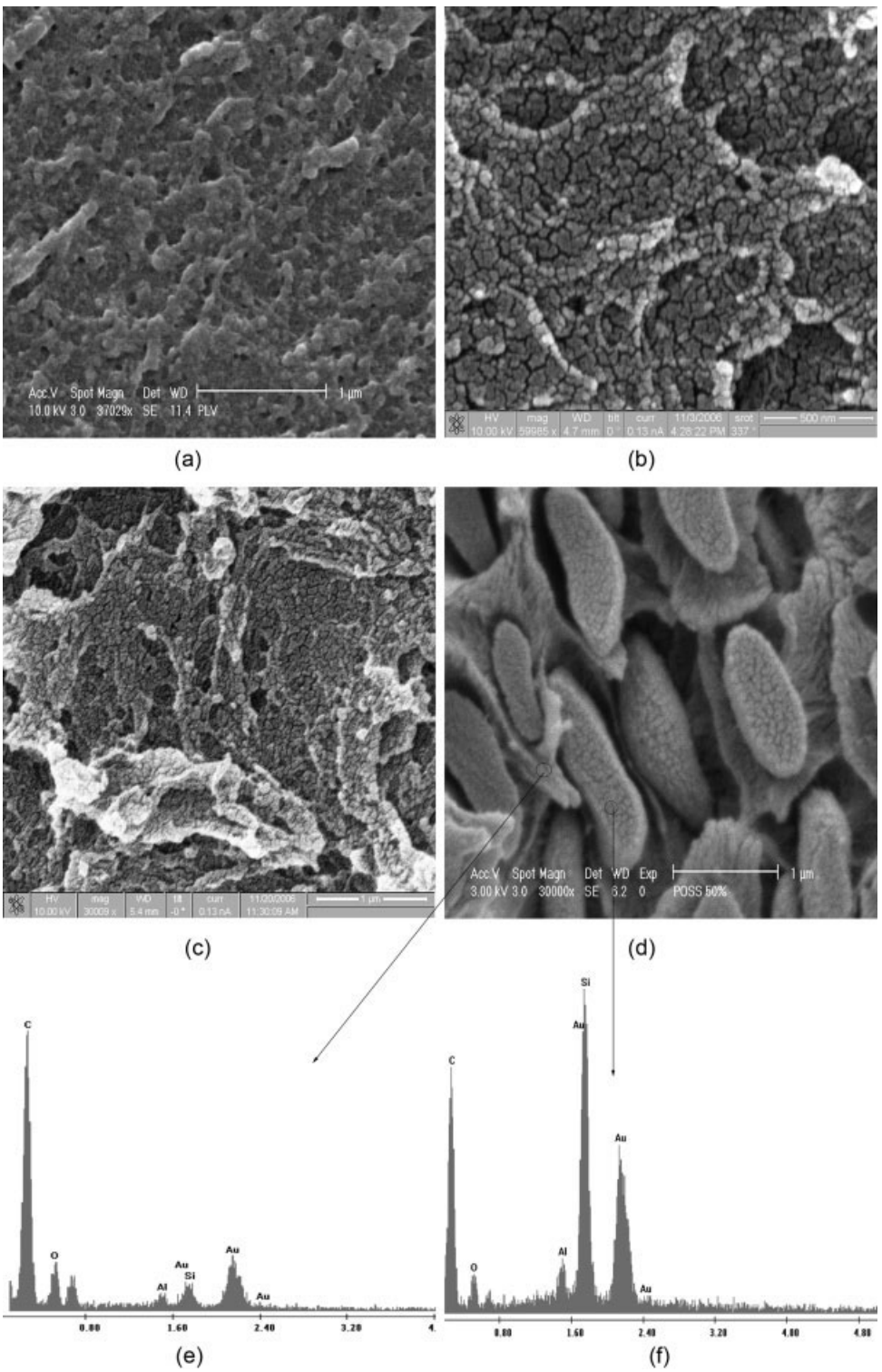

Figure 3 SEM micrographs of (a) pure PI, (b) a 10 wt % PI–OAPS composite, (c) a 20 wt % PI–OAPS composite, and (d) a 50 wt % PI–OAPS composite and EDS spectra of (e) a 50 wt % PI–OAPS composite with polymer focus and (f) a PI–POSS 50 wt % composite with aggregate focus.

50 wt % PI–OAPS composites are shown in Figure 3(a–d), respectively. The pure PI and 20 and 50 wt % composite SEM images are at a 1-μm resolution, whereas the image of the 10 wt % composite is at a resolution of 500 nm. The 10 and 20 wt % micrographs show a uniform cross section with no visible phase separation and look similar to the fracture surface of pure PI. The SEM micrograph of the 50 wt %

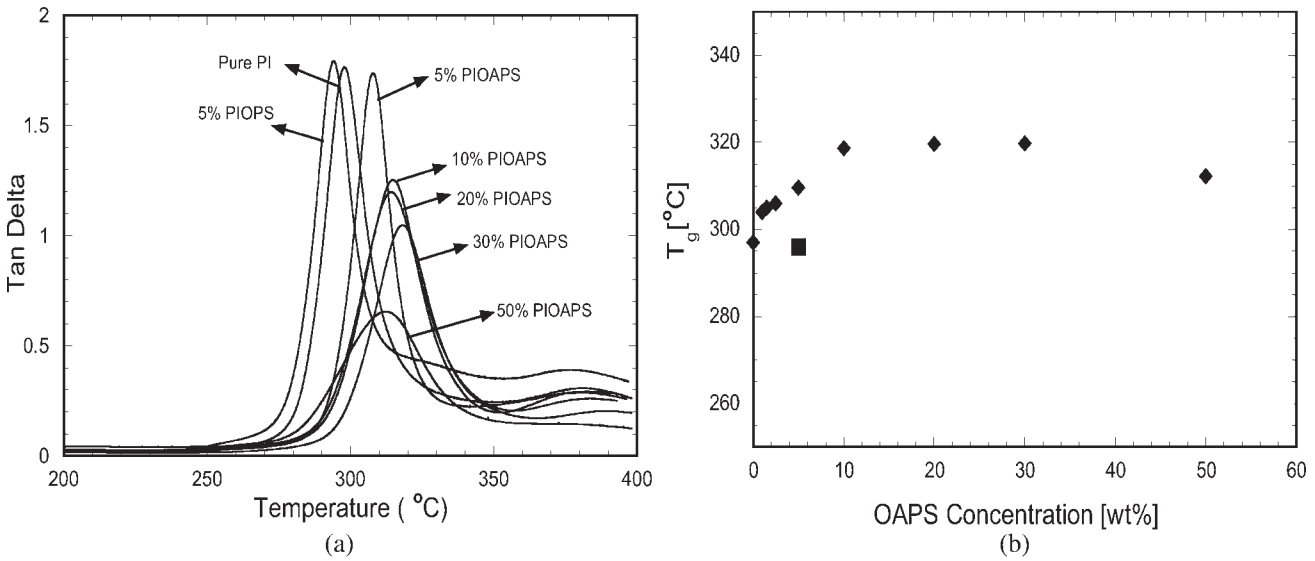

Figure 4 (a) Tan δ curves of pure PI, PI–OPS, and PI–OAPS with different concentrations of OAPS over a narrow temperature range and (b) changes in T_g determined from the peak of the tan δ curves: (◆) PI–OAPS composite and (■) 5 wt % PI–OPS composite.

composite shows distinct phase separation with the formation of a regular array of micrometer-size aggregates. A similar fracture surface with silica-rich domains was observed by Wahab and coworkers[12,19] for a 30 wt % hybrid composite of PI and polyvinylsilsesquioxane. They also observed that in comparison with another commonly used sol–gel precursor tetraethyl orthosilicate (TEOS), the organic polyvinylsilsesquioxane produced better interfacial interactions and enhanced properties. For this study, the energy-dispersive spectrometry (EDS) spectra of a spot of the bulk polymer matrix and the aggregates were used to probe the chemical nature of the aggregates [Fig. 3(e,f)]. Qualitative peak identification revealed a high Si concentration in the aggregates in comparison with the bulk polymer. A gold peak appeared in the EDS spectrum as the samples were gold-coated during sample preparation. The presence of a strong carbon peak in Figure 3(f) suggests that there may be some entrapped polymer in this region. This suggests that the polymer may act as a binder to bring these particles together to form such nanosized particles within the polymer matrix.

Thus, the SEM study suggests that OAPS has very favorable interactions with the PI matrix up to a 20 wt % loading. Although there is the formation of a regular distribution of larger particles of OAPS with some trapped PI at 50 wt %, the particles seem to be in close contact with the polymer. This confirms that amine functionalization significantly aids in the formation of good PI–POSS composites. There is also potential for controlled formation of particles within the polymer matrix, with some polymer trapped in these aggregates to improve interfacial interactions and reduce gap formation, this being critical for many applications.

DMA

DMA was used to determine the thermal and mechanical properties of pure PI and the composite films as a function of temperature. Shifts in the location and width of the tan δ peak can be used as a measure of the extent of interaction between the polymer matrix and the filler.[20] A strong interaction with a rigid inorganic filler will typically lead to an increase in T_g, whereas a weak interaction can cause T_g to decrease.[19,20] Because OAPS is a rigid molecular-scale filler, incorporation and dispersion within the PI matrix are expected to have an impact on the polymer chain rigidity. A plot of tan δ versus the temperature is shown in Figure 4(a). T_g was determined from the peak of the tan δ curve. There was a shift in the peak to higher temperatures with an increase in the OAPS concentration up to 30 wt %. Distinctive peak broadening of the tan δ curve was also observed for the composites containing OAPS at concentrations of 20 wt % and higher. As shown in Figure 4(b), there was a gradual increase in T_g as the OAPS concentration approached 10 wt %. Beyond 10 wt %, T_g remained constant up to 30 wt % and exhibited a slight decrease at 50 wt %. There was a decrease in T_g for the 5 wt % PI–OPS composite, which may have been due to an increase in the localized free volume in the gap near the OPS surface, which would result in greater chain mobility.

The shift in T_g to higher temperatures suggests that the segmental chain mobility was restricted by

the interactions between the flexible polymer and the rigid inorganic POSS. For higher concentrations of OAPS (20 and 30 wt %), T_g did not change; however, a reduction in the peak height and peak broadening was observed. Xiong et al.[20] attributed such tan δ peak broadening and decreased peak height in a titania-containing acrylic resin to an increase in the entrapment of polymer chains within inorganic networks, resulting in a reduction of polymer chain mobility.[20] In addition to the physical entrapment of the polymer chains, the positive interactions of amines on OAPS with the PI matrix can also result in a local reduction in chain mobility.

A distribution of such interactions within a polymer matrix results in broadening of the glass-transition behavior. The decrease in T_g and peak broadening for 50 wt % PI–OAPS can be attributed to phase separation, which leads to the formation of two populations of polymers within the composite, one trapped in the POSS aggregates and the other the bulk polymer. The polymer chains in the bulk matrix are expected to be less rigid than those entrapped in the POSS aggregates, and this leads to a short, broad peak. In general, the results for DMA agree with the SEM observations, which suggest that the distribution of OAPS into the PI matrix is uniform, with visible phase separation occurring only when the concentration reaches 50 wt %. The impact of OAPS on the storage modulus is discussed in the Mechanical Testing section along with Instron tensile testing.

Thermal stability analysis of the composites

The thermal stability of the POSS molecules, pure PI, and composite films was determined with TGA in a nitrogen atmosphere. The thermal degradation behaviors of OPS, ONPS, and OAPS in nitrogen are presented in the form of derivative thermogravimetry (DTG) curves in Figure 5. The DTG peaks at 420 and 380°C suggest rapid decomposition of OPS and ONPS within a narrow temperature range. In contrast, the broad peak of OAPS from 300 to 650°C suggests that it undergoes very slow degradation.

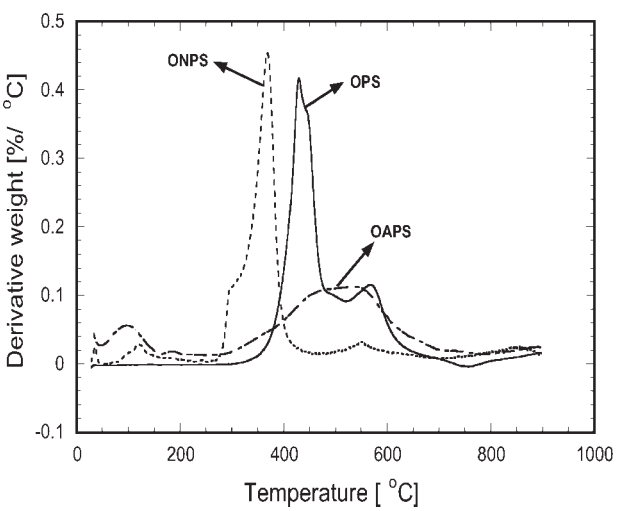

Figure 5 Thermal decomposition of (—) OPS, (- - -) ONPS, and (– - –) OAPS in a nitrogen atmosphere.

TABLE I
Changes in the Onset Decomposition Temperature of PI with Increasing OAPS Composition Measured Under a Nitrogen Atmosphere

Film	Onset decomposition temperature (°C)
Plain PI	504
5 wt % PI–OAPS	508
10 wt % PI–OAPS	508
20 wt % PI–OAPS	509
50 wt % PI–OAPS	478

The total mass loss for OPS, ONPS, and OAPS is very similar at 38%. There is some residual solvent in OAPS that contributes to the total mass loss; therefore, the mass loss of OAPS alone is effectively less than that of OPS or ONPS. The mass loss in OPS, ONPS, and OAPS is primarily due to the degradation of the functional groups (—NO_2 and —NH_2) and partial degradation of the phenyl groups. The Si—O cage in all these cases is stable up to 1000°C.[21] Therefore, it is expected that the incorporation of OAPS into a polymer matrix may improve the thermal stability of the composite.

To determine the effect of the addition of OAPS on the thermal stability of PI, TGA of pure PI was compared with that of blended PI–OAPS films in nitrogen. The onset decomposition temperatures obtained from the curve of the mass loss (%) versus the temperature are listed in Table I for the various OAPS concentrations (wt %) in the PI films. The pure PI showed decomposition in the range of 480–700°C with an onset temperature of 504°C under a nitrogen atmosphere. On the addition of 5 wt % OAPS, the decomposition temperature increased by ~ 4 to 508°C. No significant shift in the decomposition temperature was observed for the 10 and 20 wt % PI–OAPS films. With a further increase in the OAPS concentration to 50 wt %, the decomposition temperature decreased by ~ 20°C.

Also, the thermal decomposition behavior of all the composites was similar to that of the pure PI, with a shift toward higher temperatures at OAPS loadings up to 20 wt %. For composites with OAPS loadings of 20 wt % and higher, a prominent peak due to the mass loss of POSS appeared in the DTG plot, indicating the beginning of phase separation. For 50 wt %, the DTG plot showed two distinct mass-loss peaks, one of the OAPS around 480°C and the other around 500°C of the PI itself.

TABLE II
Mechanical Properties of Pure PI and PI–OAPS Composites

Film	Storage modulus (MPa)[a]	Young's modulus (MPa)	Strength (MPa)	Strain at yield (mm/mm)
Plain PI	2800 ± 136	2900 ± 74	103 ± 5	0.064 ± 0.004
1 wt % PI–OAPS	2500 ± 326	3100 ± 100	108 ± 3	0.068 ± 0.003
1.5 wt % PI–OAPS	2500 ± 57	3100 ± 58	103 ± 2	0.064 ± 0.002
2.5 wt % PI–OAPS	—	3000 ± 100	106 ± 5	0.064 ± 0.003
5 wt % PI–OAPS	2900 ± 133	3100 ± 68	105 ± 1	0.065 ± 0.002
10 wt % PI–OAPS	2500 ± 293	3200 ± 72	105 ± 2	0.056 ± 0.001
20 wt % PI–OAPS	2700 ± 89	3100 ± 46	104 ± 4	0.05 ± 0.002

[a] Measured with DMA.

Strong interactions between the thermally stable Si—O cage and the PI matrix caused the onset decomposition temperature to increase. However, this prominent change was observed primarily in the 5 wt % film as the effect of the addition of the filler is known to be more significant at lower filler concentrations. As the POSS concentration increased to 50 wt %, the onset decomposition temperature decreased as phase separation took place. The onset decomposition temperature lay between those of the pure PI and OAPS itself. Huang et al.[17] reported a 25°C increase in the decomposition temperature for an *in situ* polymerized PI–POSS system. It was attributed to the thermal stability of POSS itself and also to the stable covalent bonds between the PI and POSS. In the case of our blended PI–POSS system, any additional thermal stability came only from POSS as there were no covalent bonds, and so we saw only a slight increase in the decomposition temperature.

Mechanical testing

Mechanical properties such as the strength, toughness, and Young's modulus were determined on an Instron tensile tester. The strength was determined from the maximum stress at yield, and the strain at yield combined with the strength was used as a measure for toughness. The storage modulus (determined from DMA), Young's modulus, strength, and strain at yield of the pure PI and composites are listed in Table II. Young's modulus, which was the initial slope of the stress–strain curve, did not change significantly with the addition of OAPS, and the strength and toughness (measured indirectly from the strain at yield) of the PI–OAPS composites up to 5 wt % were comparable to those of the pure PI. However, for OAPS concentrations beyond 5 wt %, the strain at yield decreased considerably at a constant yield stress, and this led to an overall decrease in toughness. In general, the addition of an inorganic filler to a polymer can weaken the inherent properties of the polymer because of the lack of favorable interactions between the two phases, which may lead to defects. For concentrations up to 5 wt %, the strength and strain at yield were retained, and this could be attributed to good interfacial adhesion and to the incorporation of nanovoids into the polymer matrix, which increased its ability to dissipate energy.[22]

The composites with higher OAPS concentrations (>5 wt %) were relatively brittle, and this was reflected in the decrease in the strain at yield. However, it should be noted that the modulus and strengths were retained even at very high filler loadings. Huang et al.[17] reported an initial increase and then a huge drop-off in the strength and modulus as the OAPS content increased in an *in situ* polymerized PI composite (for an amine group ratio > 0.1). A study on polycarbonate–POSS composites by Zhao and Schirald[4] suggested no significant mechanical property enhancements in composites up to 10 wt % POSS.[4] It can be concluded from this mechanical study that although the composites formed by simple blending of POSS with PI do not have enhanced properties, unlike previous studies, they surely retain the superior properties of PI up to high POSS loadings.

CONCLUSIONS

Nanocomposites of PI–POSS were prepared by the conventional blending of amine-functionalized POSS with a high-temperature PI. Functionalization of OPS with amine groups enhanced the solubility in the casting solvent and in the polymer matrix. The resulting composites showed good thermal and mechanical stability. Higher T_g values of PI–OAPS composites suggest good interactions between the flexible polymer and the rigid POSS. A simple blending technique can produce transparent composites with well-dispersed POSS even at higher POSS loadings. The composites have good thermal stability up to a 20 wt % POSS loading and also retain the good mechanical properties of PI.

The authors are grateful to Joseph Lawrence of the Department of Chemical and Environmental Engineering, University of Toledo, for his assistance in obtaining scanning electron microscopy images. The authors also thank Rahul Khupse of the Department of Medicinal and Biological Chemistry, University of Toledo, and Ganesh Iyer of the Department of Chemical and Environmental Engineering, University of Toledo, for their advice on the synthesis of octaaminophenyl silsesquioxane.

References

1. Chaudhary, R.; Kar, S.; Ha, S. Polymeric Nanostructures and their Applications 2007, 2, 202.
2. Gao, Y.; He, P.; Lian, J.; Schulz, M.; Mark, J.; Zhao, J.; Wang, W.; Wang, X.; Zhang, J.; Zhou, X.; Shi, D. J Appl Polym Sci 2007, 103, 3792.
3. Li, G.; Wang, L.; Ni, H.; Pittma, C. U., Jr. J Inorg Organomet Polym 2001, 11, 123.
4. Zhao, Y.; Schirald, D. A. Polymer 2005, 46, 11640.
5. Liu, H.; Zheng, S. Macromol Rapid Commun 2005, 26, 196.
6. Ni, Y.; Zheng, S. Macromol Chem Phys 2005, 206, 2075.
7. Mittal, K. L. Polyimide: Synthesis, Characterization and Applications; Plenum: New York, 1984.
8. Lee, Y. J.; Huang, J. M.; Kuo, S. W.; Lu, J. S.; Chang, F. C. Polymer 2005, 46, 173.
9. Vu, D. Q.; Koros, W.; Stephen, M. J Membr Sci 2003, 211, 311.
10. Zimmerman, C. M.; Singh, A.; Koros, W. J Membr Sci 1997, 1137, 145.
11. Gorga, R. E.; Lau, K. S.; Gleason, K. K.; Cohen, R. E. J Appl Polym Sci 2006, 102, 1413.
12. Wahab, M. A.; Cho, W. J.; Ha, C. S. Mol Cryst Liq Cryst 2004, 417, 127.
13. Brunsvold, A. L.; Minton, T. K.; Gouzman, I.; Grossman, E.; Gonzalez, R. High Perform Polym 2004, 16, 303.
14. Domniguez, R. H.; Trevino, R. F.; Reyes, C. R.; Montiel, G. A. J Membr Sci 2006, 71, 94.
15. Tamaki, R.; Choi, J.; Laine, R. M. Chem Mater 2003, 15, 793.
16. Tamaki, R.; Tanaka, Y.; Asuncion, M. Z.; Choi, J.; Laine, R. M. J Am Chem Soc 2001, 123, 12416.
17. Huang, J. C.; He, C. B.; Xiao, Y. X.; Mya, K.; Dai, J.; Siow, Y. Polymer 2003, 44, 4491.
18. Husk, R. G.; Cassidy, P. E.; Gebert, K. L. Macromolecules 1988, 21, 1234.
19. Wahab, M. A.; Kim, I.; Ha, C. S. Polymer 2003, 44, 4705.
20. Xiong, M.; You, B.; Shuxue, Z.; Limin, W. Polymer 2004, 45, 2967.
21. Fina, A.; Tabuani, D.; Frache, A.; Boccaleri, E.; Camino, G. Thermochim Acta 2006, 440, 36.
22. Huang, J.; Poh, C.; Shen, L.; Pallathadka, P.; Zeng, K.; He, C. Acta Mater 2005, 53, 2395.